
DReSS: Data-driven Regularized Structured Streamlining for Large Language Models

Mingkuan Feng^{*1} Jinyang Wu^{*1} Shuai Zhang¹ Pengpeng Shao¹ Ruihan Jin¹ Zhengqi Wen² Jianhua Tao¹
Feihu Che¹

Abstract

Large language models (LLMs) have achieved significant progress across various domains, but their increasing scale leads to high computational and memory costs. Recent studies show that LLMs exhibit sparsity, which can be exploited for pruning. However, existing pruning methods typically follow a prune-then-finetune paradigm. Since the pruned components still contain valuable information, their direct removal often leads to irreversible performance degradation, necessitating expensive fine-tuning to recover performance. To address this, we propose a new paradigm: first apply regularization, then prune, and finally fine-tune. Based on this paradigm, we introduce DReSS, a simple and effective **Data-driven Regularized Structured Streamlining** method for LLMs. By leveraging a small amount of data to regularize the components before pruning, DReSS transfers the important information to the remaining parts of the model in advance. Compared to direct pruning, this can reduce the information loss caused by parameter removal, thereby enhancing its language modeling capabilities. Experimental results demonstrate DReSS achieves comparable performance to conventional methods even without fine-tuning, drastically alleviating computational costs. Moreover, DReSS significantly outperforms existing pruning methods even under extreme pruning ratios, significantly reducing latency and increasing throughput.

1. Introduction

Large language models (LLMs) have achieved significant advancements across a wide range of tasks and domains,

^{*}Equal contribution ¹Department of Automation, Tsinghua University, Beijing, China ²Beijing National Research Center for Information Science and Technology, Beijing, China. Correspondence to: Shuai Zhang <zhang_shuai@mail.tsinghua.edu.cn>, Jianhua Tao <jhtaoo@tsinghua.edu.cn>.

Preprint

demonstrating their robust capabilities (Zhang et al., 2022; Achiam et al., 2023; Touvron et al., 2023; Wu et al., 2024). However, as the model size increases, the growing number of parameters leads to significant computational and memory requirements, which significantly hinder the practical deployment of LLMs. Consequently, it is urgent to develop methods that can reduce model size while maintaining performance.

To address these challenges, several methods have been proposed, including pruning (Frantar & Alistarh, 2023; Sun et al., 2023; Ma et al., 2023; An et al., 2024), quantization (Frantar et al., 2022; Xiao et al., 2023), knowledge distillation (Shridhar et al., 2022; Hsieh et al., 2023), and low-rank decomposition (Saha et al., 2023). In this work, we mainly focus on pruning—an efficient and highly generalizable approach that can be seamlessly integrated with other model compression strategies. Pruning techniques are generally classified into two primary categories: unstructured pruning (Frantar & Alistarh, 2023; Sun et al., 2023) and structured pruning (Ma et al., 2023; An et al., 2024). Compared to unstructured pruning, structured pruning offers the flexibility to do recovery fine-tuning (RFT) for specific downstream tasks without relying on specialized hardware (Zhu et al., 2024). Moreover, the model obtained through structured pruning typically achieves much faster inference speed due to the regular data patterns.

Despite these advancements, existing structured pruning methods still have some limitations. They all follow the paradigm of first selecting channels or layers to prune based on a designed metric, and then performing RFT (Chavan et al., 2024). However, they neglect the fact that important information can also exist in the pruned parts (Dettmers et al., 2022; Xiao et al., 2023; Yin et al., 2023), and directly removing them leads to an irreversible decline in model performance. Thus, achieving satisfactory performance with pruned models often requires extensive data for RFT (Ma et al., 2023), increasing computational costs. Additionally, high pruning ratios frequently cause performance collapse, limiting their effectiveness in reducing latency and improving throughput.

To tackle these limitations, in this paper, we propose a new

pruning paradigm that first applies regularization to the components to be pruned, then removes those parameters, and finally performs RFT. To the best of our knowledge, we are the first to propose this paradigm. The regularization process explicitly transfers important information from the parts to be pruned to the remaining parts, thereby reducing the information loss caused by direct parameter removal. Based on this paradigm, we introduce DReSS, a **Data-driven Regularized Structured Streamlining** method for LLMs. The comparison of the proposed method with existing channel-wise pruning approaches is shown in Figure 1. Specifically, the process of DReSS is divided into the following steps: (1) select data for pre-pruning regularization and post-pruning RFT, (2) apply regularization to the selected channels in the parameter matrix, and (3) prune the specified channels, finally (4) do RFT. *First*, we randomly select a small subset of data from widely used benchmark datasets. Since the amount of selected data is small, the overhead in the regularization and RFT process can be significantly reduced. *Second*, we determine the channels to be pruned based on the pruning ratio, and apply regularization to these channels using the selected data. This redistributes important information to the unpruned components, thereby significantly mitigating performance degradation caused by direct pruning. As a result, the model can maintain robust performance even at high pruning ratios, facilitating a substantial speedup in inference. *Third*, we prune the parameters that have been regularized. *Finally*, we perform RFT on the pruned model using a small subset of samples selected in the first step. Extensive experiments show that DReSS significantly outperforms existing pruning methods in perplexity and accuracy across various pruning ratios, even without RFT, while also greatly enhancing inference speed. The main contributions of our work are summarized as follows:

- **Propose A New Paradigm:** By sequentially applying regularization, pruning, and RFT, DReSS minimizes information loss caused by direct parameter removal, thereby improving the model’s language modeling capabilities and reducing the computational cost of RFT.
- **High Performance:** DReSS surpasses existing structured pruning methods in both generation and zero-shot tasks. The pruned model achieves a substantial increase in throughput and a significant reduction in latency compared to the dense model.
- **Low Overhead:** By leveraging only a small amount of data for regularization and optional RFT, DReSS incurs minimal overhead.

2. Related Works

2.1. Pruning Methods

The elimination of redundant weights, referred to as pruning, has been an effective approach for reducing the complexity of deep neural networks over the past several decades (LeCun et al., 1989; Hassibi et al., 1993; Han et al., 2015; Wen et al., 2016; Louizos et al., 2017). Pruning methods can be broadly categorized into two types: unstructured pruning (Kurtic et al., 2022; Zhang et al., 2024; Xu et al., 2024) and structured pruning (Xia et al., 2023b; Gao et al., 2024b; Yang et al., 2024).

Unstructured pruning methods remove individual weights based on their importance. For instance, Magnitude (Han et al., 2015; Zhou et al., 2021) assumes larger weights are more important, Wanda (Sun et al., 2023) uses the product of layer weights and activations as the metric, and SparseGPT (Frantar & Alistarh, 2023) relies on the weight squared divided by the inverse Hessian matrix. The main advantage is flexibility, enabling the removal of unimportant weights while retaining critical ones, allowing high sparsity in LLMs. However, its limitations include the requirement for specialized hardware to accelerate inference (Xia et al., 2023a), the necessity for high sparsity to achieve substantial acceleration (Wang, 2020), and the inability to perform RFT on downstream tasks.

Structured pruning methods, including channel-wise pruning (An et al., 2024) and layer-wise pruning (Men et al., 2024), can achieve significant inference speedup with a low sparsity. Channel-wise pruning methods typically design a metric to evaluate the importance of channels in the parameter matrix of LLMs and then prune the less important channels. For instance, SliceGPT (Ashkboos et al., 2024) adopts Principal Component Analysis (PCA), using the eigenvalues of the covariance matrix of activation values as a metric to preserve channels corresponding to larger eigenvalues. LLM Surgeon (van der Ouderaa et al., 2023) periodically updates model weights and structures, pruning more aggressively in the initial layers and less so in the intermediate layers. Layer-wise pruning methods, such as SLEB (Song et al., 2024), iteratively prune entire transformer layers by assessing their importance. However, these methods have a key limitation: even less important channels or layers may contain valuable information, and pruning them directly often leads to significant performance degradation. To address this, we investigate the possibility of ‘shifting’ important information from the pruned parts to the retained parts, which could substantially improve model performance.

2.2. Regularization

Regularization is widely employed in machine learning (Holler & Kennard, 1970; Poggio et al., 1987; Balestriero et al.,

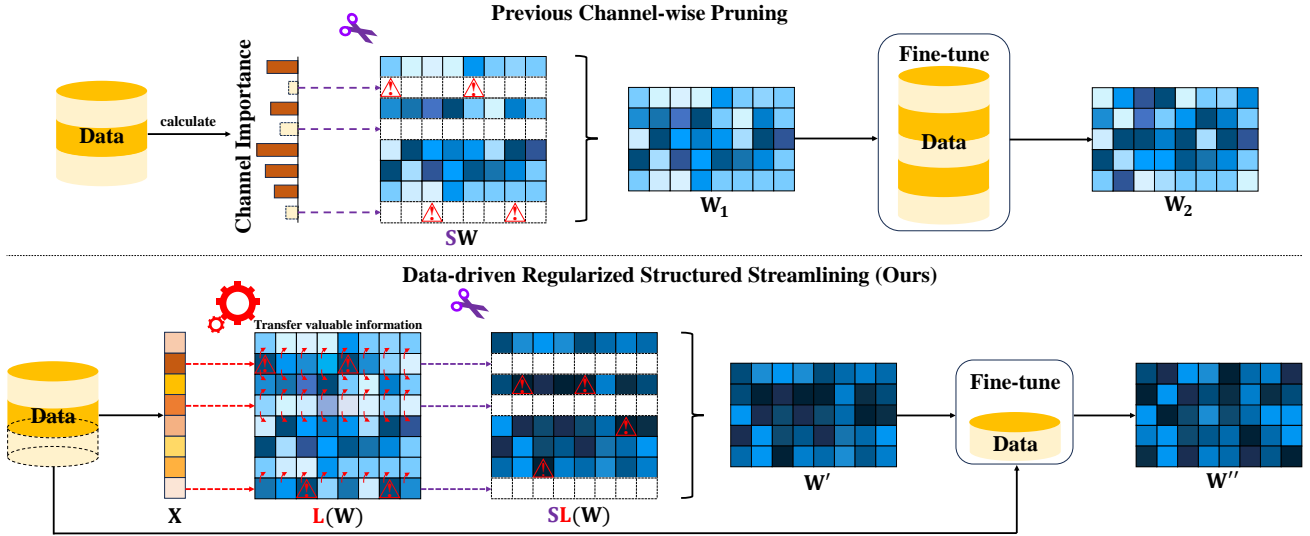


Figure 1. A comparison between existing channel-wise structured pruning methods and DReSS. The deeper blue square represents greater performance impact; the red exclamation mark indicates the important information. The taller orange-yellow cylinder represents larger data volume. $L(\cdot)$ represents the regularization, and S represents pruning. **Above**: Existing methods first select channels based on importance, followed by pruning and RFT on the pruned model. **Below**: DReSS first regularizes channels to transfer important information, prunes the channels, then do RFT with a little amount of data.

2022), such as feature selection (Tibshirani, 1996) and preventing model overfitting (Santos & Papa, 2022). The ℓ_1 -norm typically induces sparsity by driving certain coefficients to zero, while ℓ_2 -norm encourages smoother solutions (Boyd & Vandenberghe, 2004). Both of them can significantly alter the distribution pattern of the data (Han et al., 2015; Tao et al., 2023). Motivated by this observation, we propose a data-driven regularization approach. By applying a small amount of data, the regularization transfers important information from the pruned parameter space to the retained parts of the model, thereby enhancing the performance of the pruned model.

3. Methodology

In this section, we provide a detailed introduction to DReSS. The overall DReSS algorithm is summarized in Algorithm 1, our method consists of four main steps:

- **Data Selection:** Select a small amount of data for pre-pruning regularization and post-pruning RFT.
- **Regularization:** Applying regularization to the selected channels of weight matrices during forward and backward propagations.
- **Pruning:** Prune the regularized portions.
- **RFT:** Perform RFT on the pruned model using the subset of data selected in the first step.

3.1. Data Selection

The required data is selected from widely used calibration datasets, including Alpaca (Taori et al., 2023), WikiText-2 (Merity et al., 2016), PTB (Marcus et al., 1993), and C4 (Raffel et al., 2020). For instance, approximately 1,000 samples are randomly selected from the WikiText-2 training dataset for pre-pruning regularization and post-pruning RFT. In Section 4.5, we analyze the impact of using different datasets.

3.2. Regularization

To provide a clearer understanding of this section, we first introduce the relevant notations. Let p denote the pruning ratio, which indicates that $p\%$ of the model’s parameters need to be pruned. The model dimension of the LLMs is represented by d , and the number of layers is denoted by l . Additionally, let $W_{emb} \in \mathbb{R}^{b \times n \times d}$ represents the data feature map, and $W_{pos} \in \mathbb{R}^{b \times n \times d}$ denotes the positional feature map, where b is the batch size and n is the number of tokens. The model weights are represented by $W \in \mathbb{R}^{d_1 \times d_2}$. Specifically, $W_Q^i \in \mathbb{R}^{d \times d_1}$, $W_K^i \in \mathbb{R}^{d \times d_1}$, $W_V^i \in \mathbb{R}^{d \times d_1}$, and $W_o^i \in \mathbb{R}^{d_1 \times d}$ represent the parameter matrices in the i th layer Attention block. Similarly, $W_{up}^i \in \mathbb{R}^{d \times d_2}$ and $W_{down}^i \in \mathbb{R}^{d_2 \times d}$ represent the parameter matrices in the i th layer FFN block. Additionally, $w_N^i \in \mathbb{R}^d$ denotes the LayerNorm vector in the i th layer, and $W_{lm} \in \mathbb{R}^{d \times b \times n}$ represents the language modeling matrix. Finally, $I \in \mathbb{R}^{d \times d}$ represents the identity matrix, let $R \in \mathbb{R}^{d \times d}$ represent a pseudo-index selection matrix, which is a diagonal matrix

Algorithm 1 DReSS algorithm.

Input: selected data X , number of layers in LLMs l , initial model W , number of regularization iterations n , norm type: flag.
if flag==1 **then**
 use Proposition 3.2 to transform problem
end if
 $X_1, X_2 \leftarrow \text{divide}(X)$
for $i = 1$ **to** n **do**
 $\tilde{\mathcal{L}}_1 \leftarrow \text{regularize}(W_{emb}, W_{pos}, X_1)$
 $\tilde{\mathcal{L}}_{att} \leftarrow 0, \tilde{\mathcal{L}}_{FFN} \leftarrow 0, \tilde{\mathcal{L}}_2 \leftarrow 0$
for $j = 1$ **to** l **do**
 $\tilde{\mathcal{L}}_{att} \leftarrow \tilde{\mathcal{L}}_{att} + \text{regularize}(W_Q^j, W_K^j, W_V^j, W_o^j, X_1)$
 $\tilde{\mathcal{L}}_{FFN} \leftarrow \tilde{\mathcal{L}}_{FFN} + \text{regularize}(W_{up}^j, W_{down}^j, X_1)$
 $\tilde{\mathcal{L}}_2 \leftarrow \tilde{\mathcal{L}}_2 + \text{regularize}(w_N^j, X_1)$
end for
 $\tilde{\mathcal{L}}_3 \leftarrow \text{regularize}(W_{lm}, X_1)$
 $\tilde{\mathcal{L}}_{remain} \leftarrow \tilde{\mathcal{L}}_1 + \tilde{\mathcal{L}}_2 + \tilde{\mathcal{L}}_3$
 $\mathcal{L}(W, X) \leftarrow \text{forward}(W, X_1)$
 $\mathcal{L}_{sum} \leftarrow \mathcal{L}(W, X) + \tilde{\mathcal{L}}_{att} + \tilde{\mathcal{L}}_{FFN} + \tilde{\mathcal{L}}_{remain}$
 update W using backpropagation algorithm
end for
 $W \leftarrow \text{Prune}(W, R)$
 $W \leftarrow \text{Optional_RFT}(W, X_2)$

consisting of $(1 - p\%) \times d$ zeros and $p\% \times d$ ones, where the ones correspond to the selected indices.

Proposition 3.1. (Dependency between the Attention Block and FFN Block. Proof in Appendix A.1). *If regularization is applied to certain columns of W_{down}^{i-1} in the $(i-1)$ th layer FFN block, then regularization must also be applied to the corresponding rows of $W_Q^i, W_K^i,$ and W_V^i in the i th layer Attention block. The same dependency applies to W_o^i and W_{up}^{i-1} .*

We illustrate the process of applying regularization within a transformer layer (Vaswani, 2017), as shown in Figure 2. Following Proposition 3.1, in the Attention block, regularization is applied to the rows of $W_Q^i, W_K^i,$ and W_V^i corresponding to the one entries in the index matrix R , as well as to the columns of W_o^i associated with these entries. Similarly, in the FFN block, regularization is enforced on the rows of W_{up}^i and the columns of W_{down}^i that correspond to the one entries in R . We also apply regularization to the remaining parts in LLMs. Specifically, for W_{emb} , regularization is enforced on the columns corresponding to the one indices in R , and the same procedure is applied to W_{pos} . For each w_N^i within every transformer layer, regularization is applied to the elements corresponding to the one indices in R . Additionally, for the final W_{lm} , due to its dependency on W_{down}^l in the FFN block of the last transformer layer, regularization is applied to the corresponding rows.

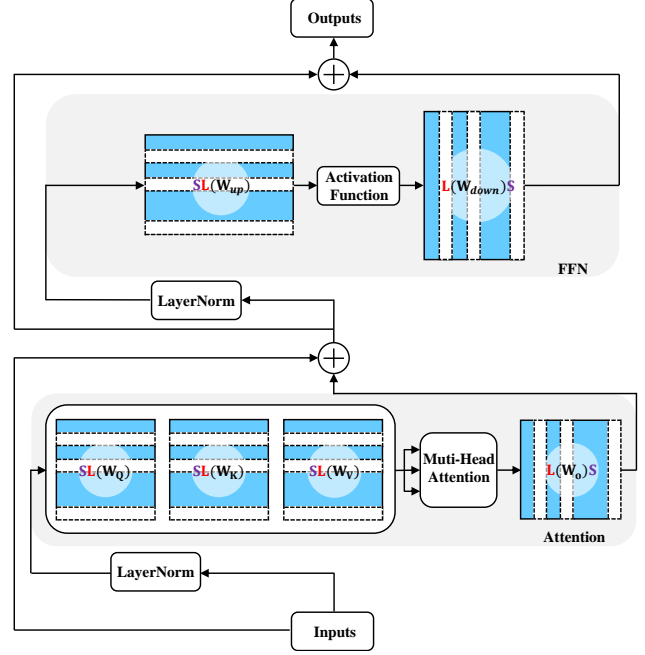


Figure 2. The pruning strategy of DReSS in a transformer layer.

Therefore, the overall loss function consists of the language modeling loss and the loss induced by regularization, which is defined below:

$$\mathcal{L}_{sum} = \mathcal{L}(W, X) + \sum_{i=1}^l \tilde{\mathcal{L}}_{att}^i + \sum_{i=1}^l \tilde{\mathcal{L}}_{FFN}^i + \tilde{\mathcal{L}}_{remain} \quad (1)$$

where $\mathcal{L}(W, X)$ denotes the language modeling loss and X is the input data, and the remaining term represents the regularization loss. $\tilde{\mathcal{L}}_{att}^i$ denotes the i th layer attention block regularization loss, which is defined as:

$$\tilde{\mathcal{L}}_{att}^i = \lambda(\|RW_Q^i\| + \|RW_K^i\| + \|RW_V^i\| + \|W_o^i R\|) \quad (2)$$

$\tilde{\mathcal{L}}_{FFN}^i$ denotes the i th layer FFN block regularization loss and the definition is as below:

$$\tilde{\mathcal{L}}_{FFN}^i = \lambda\|RW_{up}^i\| + \lambda\|W_{down}^i R\| \quad (3)$$

$\tilde{\mathcal{L}}_{remain}$ denotes the remaining parts of the LLMs' regularization loss as follows:

$$\tilde{\mathcal{L}}_{remain} = \lambda(\|W_{emb} R\| + \|W_{pos} R\| + \sum_{i=1}^l \|R w_N^i\| + \|RW_{lm}\|) \quad (4)$$

In Equations 2, 3, and 4, $\|\cdot\|$ represents a certain vector norm applied to the matrix column-wise.

Proposition 3.2. (If the loss function includes the ℓ_1 -norm, it can also be solved using backpropagation. Proof in Appendix A.2). *The following unconstrained optimization problem is equivalent to the constrained optimization problem, where $\|\cdot\|_1$ denotes the ℓ_1 -norm.*

$$\begin{aligned} \min \|x\|_1 &\iff \min_{x,y} \mathbf{1}^T y \\ \text{s.t.} & -y \leq x \leq y, \\ & y \geq 0. \end{aligned} \quad (5)$$

We formalize the minimization of the overall loss as an optimization problem. When ℓ_2 -norm is used, the problem can be efficiently solved using backpropagation (BP) algorithm (Rumelhart et al., 1986). In contrast, when the ℓ_1 -norm is employed, as the regularization losses introduced by various components in LLMs are similar, we consider only $\tilde{\mathcal{L}}_{\text{FFN}}^i$ as an example. According to Proposition 3.2, the optimization problem in Equation 6 can be equivalently transformed into a constrained formulation in Equation 7, enabling its solution by BP algorithm.

$$\min_W \mathcal{L}(W, X) + \lambda \|RW_{up}^i\|_1 + \lambda \|W_{down}^i R\|_1 \quad (6)$$

$$\begin{aligned} \min_{W, Y_1, Y_2} \mathcal{L}(W, X) + \mathbf{1}^T Y_1 \mathbf{1} + \mathbf{1}^T Y_2 \mathbf{1} \\ \text{s.t.} \quad & -Y_1 \leq RW_{up}^i \leq Y_1, \\ & -Y_2 \leq W_{down}^i R \leq Y_2, \\ & Y_1 \geq 0, \quad Y_2 \geq 0. \end{aligned} \quad (7)$$

During the forward and backward propagation processes, due to the application of regularization on certain specific channels in LLMs, the values within these rows or columns are significantly reduced. Intuitively, this reduction could potentially transfer important information and decrease the impact of these parameters on the model’s performance.

3.3. Pruning

After completing the regularization, we prune the rows and columns directly using the pseudo-index selection matrix R . For clarity, we define $S = I - R$ and the pruning for the i th layer attention block is then performed as:

$$\begin{aligned} W_Q^{i'} &= SW_Q^i, & W_K^{i'} &= SW_K^i \\ W_V^{i'} &= SW_V^i, & W_o^{i'} &= W_o^i S \end{aligned} \quad (8)$$

While for the FFN block, it follows:

$$W_{up}^{i'} = SW_{up}^i, \quad W_{down}^{i'} = W_{down}^i S \quad (9)$$

The remaining parts are pruned as below:

$$\begin{aligned} W_{emb}^{i'} &= W_{emb}^i S, & W_{pos}^{i'} &= W_{pos}^i S \\ w_N^{i'} &= Sw_N^i, & W_{lm}^{i'} &= SW_{lm}^i \end{aligned} \quad (10)$$

The entire pruning process is straightforward and simple.

3.4. Optional RFT

After pruning, we perform RFT on the model using a small subset of the data selected in Section 3.1, leveraging LoRA (Hu et al., 2021). This step is optional, as experimental results in section 4.7 show that DReSS without RFT still maintains competitive performance in terms of both perplexity and zero-shot accuracy.

4. Experiments

This section introduces experimental setup (4.1) and analyzes the effectiveness of DReSS from the following aspects: performance comparison (4.2), acceleration (4.3), robustness under different pruning ratios (4.4), dependency on different datasets (4.5), low overhead (4.6), and ablation study (4.7).

4.1. Experimental Setup

Implementation: DReSS and baseline methods are implemented on the PyTorch framework (Paszke et al., 2019), utilizing the Hugging Face Transformers library (Wolf, 2019). All experiments are conducted on 80GB NVIDIA A100 GPUs. For fairness, we use llm-eval-harness (Gao et al., 2024a) to evaluate the pruned models. More details are shown in Appendix B.

Datasets: To evaluate the performance of DReSS, we conducted experiments on generation and zero-shot tasks. For generation task, following prior work (Ashkboos et al., 2024), we evaluate the model’s perplexity on WikiText-2. For zero-shot task evaluation, the benchmarks consists of PIQA (Bisk et al., 2020), WinoGrande (Sakaguchi et al., 2021), HellaSwag (Zellers et al., 2019), ARC-e and ARC-c (Clark et al., 2018). To demonstrate that DReSS is not specifically dependent on the regularization data, we use a randomly selected subset of data from Alpaca (Taori et al., 2023), WikiText-2 (Merity et al., 2016), PTB (Marcus et al., 1993), and C4 (Raffel et al., 2020) for calibration before pruning and for RFT after pruning.

Models: The models pruned using DReSS include the LLaMA models (LLaMA2-7B, LLaMA2-13B) (Touvron et al., 2023), OPT models (OPT-2.7B, OPT-6.7B, OPT-13B) (Zhang et al., 2022), and Phi-2 (Javaheripi et al., 2023).

Baselines: We evaluate DReSS against competitive structured pruning methods: LLM Surgeon (van der Ouderaa et al., 2023), SliceGPT (Ashkboos et al., 2024), and SLEB (Song et al., 2024). Among them, LLM Surgeon and SliceGPT are channel-wise, SLEB is layer-wise. To ensure a fair comparison, in the subsequent experiments, we ensure that the data used for regularization in DReSS is consistent with the calibration data used by LLM Surgeon, SliceGPT, and SLEB before pruning, and that the data

Table 1. Performance comparison of different pruning methods. ‘PPL’ refers to the perplexity on WikiText-2. The accuracy is reported on five zero-shot tasks: PIQA, WinoGrande, HellaSwag, ARC-e, and ARC-c, as well as the average accuracy. The best result is highlighted in **bold**, and the second-best in underlined. DReSS- ℓ_2 denotes the use of the ℓ_2 -norm, while DReSS- ℓ_1 denotes the use of the ℓ_1 -norm.

Model	Method	Pruning Ratio	PPL (\downarrow)	PIQA	WinoGrande	HellaSwag	ARC-e	ARC-c	Avg_Acc
Phi-2	Dense	0%	5.28	79.11	75.77	73.83	78.32	54.18	72.24
	LLM Surgeon	25%	7.26	67.28	63.25	54.24	51.62	35.85	54.44
	SliceGPT	25%	7.08	69.21	65.35	52.40	53.70	31.66	54.46
	SLEB	25%	7.82	67.94	62.79	49.80	48.55	29.34	51.68
	DReSS- ℓ_2	25%	6.25	<u>68.52</u>	66.71	<u>56.73</u>	<u>52.78</u>	37.63	56.47
	DReSS- ℓ_1	25%	<u>6.28</u>	<u>68.67</u>	<u>65.32</u>	57.16	<u>52.39</u>	<u>37.28</u>	<u>56.16</u>
OPT-2.7B	Dense	0%	12.46	74.81	61.01	60.58	54.42	31.14	56.39
	LLM Surgeon	25%	12.60	68.22	58.06	46.25	<u>51.52</u>	27.31	50.27
	SliceGPT	25%	14.56	65.29	57.22	47.85	49.79	27.99	49.63
	SLEB	25%	16.73	63.28	55.37	43.09	45.62	24.21	46.31
	DReSS- ℓ_2	25%	<u>12.52</u>	69.12	58.98	49.10	50.62	28.15	51.20
	DReSS- ℓ_1	25%	12.48	<u>68.89</u>	<u>58.33</u>	<u>48.62</u>	51.67	<u>27.55</u>	<u>51.01</u>
OPT-6.7B	Dense	0%	10.85	76.39	65.19	67.16	60.14	34.64	60.70
	LLM Surgeon	25%	<u>11.33</u>	72.12	61.08	62.36	54.19	30.52	56.05
	SliceGPT	25%	11.90	70.35	60.62	58.15	52.78	29.52	54.28
	SLEB	25%	13.80	71.28	60.96	59.26	51.54	29.83	54.57
	DReSS- ℓ_2	25%	11.06	74.26	<u>63.12</u>	<u>61.26</u>	56.64	<u>31.77</u>	57.41
	DReSS- ℓ_1	25%	11.74	<u>73.86</u>	64.28	60.45	<u>56.36</u>	32.07	<u>57.40</u>
OPT-13B	Dense	0%	10.12	76.82	64.80	69.81	61.87	35.67	61.79
	LLM Surgeon	25%	11.02	74.18	64.33	65.37	60.96	34.98	59.96
	SliceGPT	25%	10.94	73.67	64.25	63.28	60.52	34.64	59.27
	SLEB	25%	12.02	72.62	63.96	62.79	59.21	34.12	58.50
	DReSS- ℓ_2	25%	10.38	<u>74.06</u>	64.57	66.82	61.56	35.33	60.47
	DReSS- ℓ_1	25%	<u>10.56</u>	<u>73.65</u>	<u>64.38</u>	<u>66.46</u>	<u>61.15</u>	34.74	<u>60.07</u>
LLaMA2-7B	Dense	0%	5.47	79.11	69.06	75.99	74.58	46.25	69.00
	LLM Surgeon	25%	7.38	70.59	<u>65.87</u>	58.66	63.65	38.33	59.42
	SliceGPT	25%	7.55	66.87	63.38	54.16	58.46	34.56	55.48
	SLEB	25%	10.24	63.25	62.36	53.77	55.82	32.24	53.49
	DReSS- ℓ_2	25%	<u>5.86</u>	<u>73.18</u>	66.49	<u>61.73</u>	65.42	40.86	61.54
	DReSS- ℓ_1	25%	5.81	73.42	65.73	61.92	<u>65.26</u>	<u>39.68</u>	<u>61.20</u>
LLaMA2-13B	Dense	0%	4.88	80.47	72.22	79.39	77.48	49.23	71.76
	LLM Surgeon	25%	5.75	77.75	69.62	74.31	72.83	43.52	67.61
	SliceGPT	25%	6.30	68.55	67.48	58.10	62.50	37.88	58.90
	SLEB	25%	7.39	66.93	65.87	55.48	60.06	35.14	56.70
	DReSS- ℓ_2	25%	5.12	76.14	71.22	<u>76.51</u>	<u>73.45</u>	46.87	68.84
	DReSS- ℓ_1	25%	5.16	<u>77.24</u>	<u>70.61</u>	76.75	73.84	<u>45.46</u>	<u>68.78</u>

used for RFT in each method is also the same. We also compared with powerful unstructured pruning methods like Mangniude (Han et al., 2015), Wanda (Sun et al., 2023), and SparseGPT (Frantar & Alistarh, 2023) and the results are in Appendix C.

Evaluation Metrics: The performance on generation task is measured by *perplexity*, a well-established and robust metric (Yao et al., 2022), while zero-shot tasks performance is evaluated using *accuracy* (Dong et al., 2024). The acceleration effects are represented by *throughput* and *latency* (Song et al., 2024).

4.2. Performance Comparison

To ensure fairness, we randomly selected 1,000 samples from WikiText-2 for each method with a sequence length of 2048. The ratio of calibration data and the RFT data was

set to 3:1, and the pruning ratio was 25%.

As shown in Table 1, DReSS demonstrates superior performance across both *generation* and *zero-shot* tasks achieving lowest perplexity and highest average accuracy across all models. For instance, on LLaMA2-7B, its perplexity is 20% lower than the second-best method, LLM Surgeon. Notably, on OPT-13B, compared to the dense model, DReSS experiences only a 1% drop in average accuracy. The performance difference between the ℓ_2 -norm and ℓ_1 -norm is tiny. In Figure 3, we present the ratio of the absolute values of model parameters and activation values after and before regularization of the selected portions. The results show that, in most intermediate layers, the parameters and activation values after regularization are reduced to 30% of their original values, which indicates that the amount of information contained in this part of the parameter space has decreased. We also present the changes occurring in

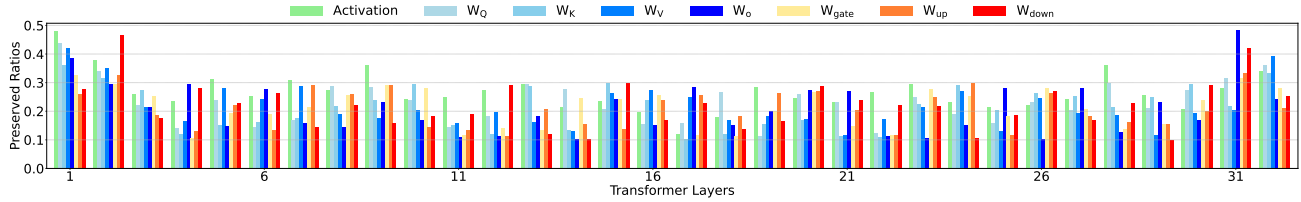


Figure 3. The ratio of the sum of absolute parameter values after regularization to that before regularization for LLaMA2-7B. For example, regularization is applied to the last 25% of rows in W_Q , and the absolute sum of these rows after regularization is divided by the sum of the corresponding rows before regularization to obtain the Preserved Ratios. This is applied similarly to other matrices such as W_K , W_V , W_O , W_{gate} , W_{up} , W_{down} , and for layer activations X , the sum of the regularized columns is compared to the original sum.

the unregularized part in Appendix D. The results show that this part has increased compared to before, indicating that it now accommodates more important information. Overall, regularization transfers important information hidden in the pruned portions to the remaining parts.

4.3. Acceleration Effectiveness

Language processing in LLMs comprises two primary stages: prompt processing, which is compute-bound, and token generation, which is memory-bound. We separately analyze the speedup achieved in each stage. Table 2 presents the throughput and latency results for OPT-13B and LLaMA2-13B, evaluated using a single NVIDIA A100 GPU. Following the methodology of previous work (Song et al., 2024), the token generation test scenario involves generating sentences of 128 tokens with a batch size of 64, whereas for prompt processing, latency is measured by processing an input sequence of 2048 tokens.

At a pruning ratio of 50% on OPT-13B, DReSS delivers a 35% improvement in throughput and a 30% reduction in latency compared to the dense model. These results highlight the superior efficiency of DReSS in accelerating model inference.

Table 2. Comparison of throughput and latency under different ratios on OPT-13B and LLaMA2-13B. ‘PPL’ refers to the perplexity on Wikitext2, ‘PR’ represents ‘pruning ratio’, ‘TI’ represents ‘throughput increase’.

Model	Method	PR	PPL(↓)	Tokens/s	TI	Latency(ms)	Speedup
OPT-13B	Dense	0%	10.12	1029	1.00×	386.5	1.00×
	DReSS	25%	10.38	1194	1.16×	319.42	1.21×
	DReSS	50%	12.15	1389	1.35×	274.11	1.41×
LLaMA2-13B	Dense	0%	4.88	1066	1.00×	396.9	1.00×
	DReSS	25%	5.12	1215	1.14×	330.8	1.20×
	DReSS	50%	7.59	1407	1.32×	285.5	1.39×

4.4. Robustness to Varying Pruning Ratios

Keeping all other settings consistent with Section 4.2, we extend the pruning ratio from 20% to 60%. The perplexity of LLaMA2-7B on WikiText-2 under different methods are shown in Figure 4. DReSS significantly outperforms

other methods across various pruning ratios. At a pruning ratio of 20%, DReSS performs similarly to the dense model. When the pruning ratio is up to 60%, SLEB collapses, while DReSS maintains relatively low perplexity compared to other pruning methods. This demonstrates that DReSS maintains robust performance even under extreme pruning ratios, enabling structured pruning to achieve high sparsity levels and unlocking significant potential for model acceleration. A more detailed exploration of pruning ratios using DReSS is provided in the Appendix E.

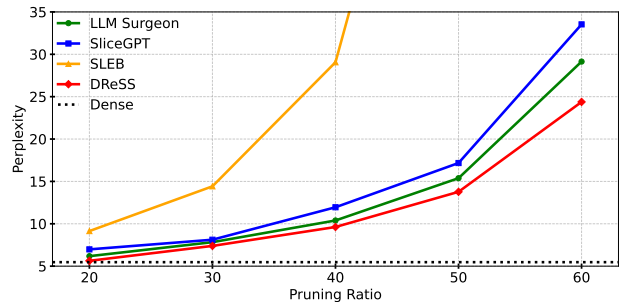


Figure 4. Perplexity of LLaMA-7B pruned by various approaches under different pruning ratios on WikiText-2.

4.5. Dependency on Datasets

Since DReSS relies on data-driven regularization, we investigate its potential dataset dependence. We evaluated perplexity for four methods on WikiText-2, using calibration and RFT data selected from Alpaca, WikiText-2, PTB, and C4. To ensure fairness, we randomly selected 1,000 samples from each dataset, with other settings consistent with Section 4.2. As shown in Figure 5, DReSS consistently outperforms the other methods across datasets, demonstrating its robustness and scalability. More details are shown in Appendix F.

4.6. Minimal Overhead

We evaluated the perplexity of each method on LLaMA2-7B using varying amounts of data, keeping all other conditions

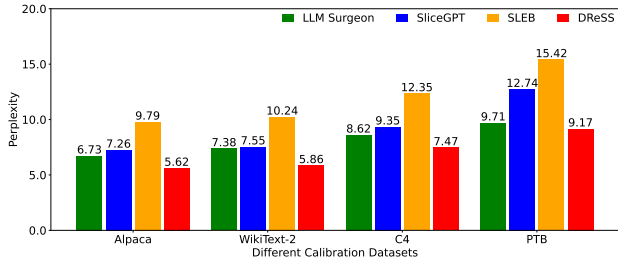


Figure 5. Comparison of perplexity on different calibration datasets at a pruning ratio of 25% on LLaMA2-7B.

consistent with Section 4.2 and only change the data size from 500 to 8,000. As shown in Table 3, when only 1,000 samples were used for regularization and RFT, DReSS outperformed the other methods that used 4,000 samples. This further highlights the effectiveness and efficiency of applying regularization prior to pruning, as it transfers critical information from the pruned segments in advance, enabling DReSS to deliver strong performance with minimal data overhead.

Table 3. The impact of the amount of data on model performance.

Data Size	500	1000	2000	4000	8000
LLM Surgeon	8.14	7.38	6.55	5.89	5.56
SliceGPT	8.63	7.55	6.82	6.07	5.74
SLEB	13.26	10.24	9.67	8.79	7.83
DReSS	6.75	5.86	5.61	5.48	5.43

4.7. Ablation Study

Effectiveness of Regularization: As shown in Table 4, both random pruning and full parameter regularization significantly increase perplexity on WikiText-2 and reduce average accuracy at a 25% pruning ratio. This highlights the importance of applying regularization exclusively to the pruned components. Additionally, RFT after pruning has minimal impact on model performance, indicating that the RFT process is optional.

Table 4. Ablation results on LLaMA2-7B and LLaMA2-13B. ‘FPR’ refers to full parameter regularization, ‘R’ refers regularization. ‘w/o’ denotes the removal of specific components.

Model	Method Setting	PPL(↓)	Δ	AVG.ACC	Δ(↓)
LLaMA2-7B	DReSS	5.86	0.00	61.54	0.00
	w FPR	12.68	+6.82	50.26	-11.28
	w/o R	22.38	+16.52	47.25	-14.29
	w/o RFT	5.97	+0.11	59.56	-1.98
LLaMA2-13B	DReSS	5.12	0.00	68.84	0.00
	w FPR	10.53	+5.41	53.28	-15.56
	w/o R	18.94	+13.82	50.17	-18.67
	w/o RFT	5.39	+0.27	67.96	-0.88

Data Ratio of Regularization and RFT: With all other settings consistent with Section 4.2, we only varied the data

Table 5. The perplexity on WikiText-2 under different regularization and RFT data ratio using LLaMA2-7B at a pruning ratio of 25%.

Ratio (R/F)	4:1	3:1	2:1	1:1	1:2	1:3
PPL(↓)	5.89	5.86	6.07	6.73	7.45	8.62

Table 6. The perplexity of different λ on LLaMA2-7B.

λ	10^{-5}	10^{-4}	10^{-3}	5×10^{-3}	10^{-2}	5×10^{-2}	10^{-1}
PPL(↓)	7.47	6.04	5.86	5.93	6.12	7.26	10.55

ratio, and the results are shown in Table 5. It can be observed that when the ratio is 3:1, the model achieves the lowest perplexity. When the ratio is 4:1, the increase in perplexity is less pronounced, but when the ratio is 1:1, the perplexity increases significantly by 15%. These results underscore the importance of the regularization process relative to the RFT applied after pruning.

Trade-Off Between Language Modeling and Regularization:

Keeping all other settings consistent with Section 4.2, we evaluate the model’s performance by varying $\lambda \in [10^{-5}, 10^{-4}, 10^{-3}, 5 \times 10^{-3}, 10^{-2}, 5 \times 10^{-2}, 10^{-1}]$. As shown in Table 6, when $\lambda = 10^{-5}$, the regularization loss is too small to effectively shift important values, leading to a significant increase in perplexity after pruning. In contrast, when $\lambda = 10^{-1}$, excessive regularization compromises the model’s language modeling ability, causing a notable performance decline post-pruning. Optimal performance is achieved at $\lambda = 10^{-3}$, demonstrating the importance of balancing language modeling loss and regularization loss for effective pruning.

5. Conclusion

In this paper, we introduce a novel pruning paradigm: first applying regularization to the pruned components, followed by pruning and then RFT. Unlike traditional paradigms that first prune based on importance and then apply RFT, DReSS transfers critical information from the pruned parameter space to the remaining components during regularization, effectively mitigating the irreversible performance degradation caused by information loss. DReSS demonstrates superior performance in both generation and zero-shot tasks, significantly outperforming existing pruning methods. For instance, DReSS surpasses the powerful LLM Surgeon by 20% in perplexity on LLaMA2-7B. On OPT-13B, with a pruning ratio of 25%, the average accuracy drops by only 1%, while achieving a 1.41x speedup compared to the dense model. Moreover, DReSS requires only 25% of the data to achieve comparable performance to previous methods, substantially reducing both data and computational costs while minimizing the reliance on RFT.

Impact Statement

Pruning plays a crucial role in model compression. DReSS is an efficient and low-overhead pruning method, which enables smaller models to achieve competitive performance, especially in resource-constrained scenarios and it also provides some insights for the development of LLMs.

References

- Achiam, J., Adler, S., Agarwal, S., Ahmad, L., Akkaya, I., Aleman, F. L., Almeida, D., Altenschmidt, J., Altman, S., Anadkat, S., et al. Gpt-4 technical report. *arXiv preprint arXiv:2303.08774*, 2023.
- An, Y., Zhao, X., Yu, T., Tang, M., and Wang, J. Fluctuation-based adaptive structured pruning for large language models. In *Proceedings of the AAAI Conference on Artificial Intelligence*, volume 38, pp. 10865–10873, 2024.
- Ashkboos, S., Croci, M. L., Nascimento, M. G. d., Hoefler, T., and Hensman, J. SliceGPT: Compress large language models by deleting rows and columns. *arXiv preprint arXiv:2401.15024*, 2024.
- Balestriero, R., Bottou, L., and LeCun, Y. The effects of regularization and data augmentation are class dependent. *Advances in Neural Information Processing Systems*, 35: 37878–37891, 2022.
- Bisk, Y., Zellers, R., Gao, J., Choi, Y., et al. Piqa: Reasoning about physical commonsense in natural language. In *Proceedings of the AAAI conference on artificial intelligence*, volume 34, pp. 7432–7439, 2020.
- Boyd, S. and Vandenberghe, L. *Convex optimization*. Cambridge university press, 2004.
- Chavan, A., Magazine, R., Kushwaha, S., Debbah, M., and Gupta, D. Faster and lighter llms: A survey on current challenges and way forward. *arXiv preprint arXiv:2402.01799*, 2024.
- Clark, P., Cowhey, I., Etzioni, O., Khot, T., Sabharwal, A., Schoenick, C., and Tafjord, O. Think you have solved question answering? try arc, the ai2 reasoning challenge. *arXiv preprint arXiv:1803.05457*, 2018.
- Dettmers, T., Lewis, M., Belkada, Y., and Zettlemoyer, L. Gpt3. int8 (): 8-bit matrix multiplication for transformers at scale. *Advances in Neural Information Processing Systems*, 35:30318–30332, 2022.
- Dong, P., Li, L., Tang, Z., Liu, X., Pan, X., Wang, Q., and Chu, X. Pruner-zero: Evolving symbolic pruning metric from scratch for large language models. *arXiv preprint arXiv:2406.02924*, 2024.
- Frantar, E. and Alistarh, D. SparseGPT: Massive language models can be accurately pruned in one-shot. In *International Conference on Machine Learning*, pp. 10323–10337. PMLR, 2023.
- Frantar, E., Ashkboos, S., Hoefler, T., and Alistarh, D. GPTQ: Accurate post-training quantization for generative pre-trained transformers. *arXiv preprint arXiv:2210.17323*, 2022.
- Gao, L., Tow, J., Abbasi, B., Biderman, S., Black, S., DiPofi, A., Foster, C., Golding, L., Hsu, J., Le Noac’h, A., Li, H., McDonnell, K., Muennighoff, N., Ociepa, C., Phang, J., Reynolds, L., Schoelkopf, H., Skowron, A., Sutawika, L., Tang, E., Thite, A., Wang, B., Wang, K., and Zou, A. A framework for few-shot language model evaluation, 07 2024a. URL <https://zenodo.org/records/12608602>.
- Gao, S., Lin, C.-H., Hua, T., Zheng, T., Shen, Y., Jin, H., and Hsu, Y.-C. Disp-LLM: Dimension-independent structural pruning for large language models. *arXiv preprint arXiv:2410.11988*, 2024b.
- Han, S., Pool, J., Tran, J., and Dally, W. Learning both weights and connections for efficient neural network. *Advances in neural information processing systems*, 28, 2015.
- Hassibi, B., Stork, D. G., and Wolff, G. J. Optimal brain surgeon and general network pruning. In *IEEE international conference on neural networks*, pp. 293–299. IEEE, 1993.
- Hoerl, A. E. and Kennard, R. W. Ridge regression: applications to nonorthogonal problems. *Technometrics*, 12(1): 69–82, 1970.
- Hsieh, C.-Y., Li, C.-L., Yeh, C.-K., Nakhost, H., Fujii, Y., Ratner, A., Krishna, R., Lee, C.-Y., and Pfister, T. Distilling step-by-step! outperforming larger language models with less training data and smaller model sizes. *arXiv preprint arXiv:2305.02301*, 2023.
- Hu, E. J., Shen, Y., Wallis, P., Allen-Zhu, Z., Li, Y., Wang, S., Wang, L., and Chen, W. Lora: Low-rank adaptation of large language models. *arXiv preprint arXiv:2106.09685*, 2021.
- Javaheripi, M., Bubeck, S., Abdin, M., Aneja, J., Bubeck, S., Mendes, C. C. T., Chen, W., Del Giorno, A., Eldan, R., Gopi, S., et al. Phi-2: The surprising power of small language models. *Microsoft Research Blog*, 1(3):3, 2023.
- Kurtic, E., Campos, D., Nguyen, T., Frantar, E., Kurtz, M., Fineran, B., Goin, M., and Alistarh, D. The optimal bert surgeon: Scalable and accurate second-order pruning for large language models. *arXiv preprint arXiv:2203.07259*, 2022.

- LeCun, Y., Denker, J., and Solla, S. Optimal brain damage. *Advances in neural information processing systems*, 2, 1989.
- Louizos, C., Welling, M., and Kingma, D. P. Learning sparse neural networks through l_0 regularization. *arXiv preprint arXiv:1712.01312*, 2017.
- Ma, X., Fang, G., and Wang, X. Llm-pruner: On the structural pruning of large language models. *Advances in neural information processing systems*, 36:21702–21720, 2023.
- Mangrulkar, S., Gugger, S., Debut, L., Belkada, Y., Paul, S., and Bossan, B. Peft: State-of-the-art parameter-efficient fine-tuning methods. URL: <https://github.com/huggingface/peft>, 2022.
- Marcus, M., Santorini, B., and Marcinkiewicz, M. A. Building a large annotated corpus of english: The penn treebank. *Computational linguistics*, 19(2):313–330, 1993.
- Men, X., Xu, M., Zhang, Q., Wang, B., Lin, H., Lu, Y., Han, X., and Chen, W. Shortgpt: Layers in large language models are more redundant than you expect. *arXiv preprint arXiv:2403.03853*, 2024.
- Merity, S., Xiong, C., Bradbury, J., and Socher, R. Pointer sentinel mixture models. *arXiv preprint arXiv:1609.07843*, 2016.
- Paszke, A., Gross, S., Massa, F., Lerer, A., Bradbury, J., Chanan, G., Killeen, T., Lin, Z., Gimelshein, N., Antiga, L., et al. Pytorch: An imperative style, high-performance deep learning library. *Advances in neural information processing systems*, 32, 2019.
- Poggio, T., Torre, V., and Koch, C. Computational vision and regularization theory. *Readings in computer vision*, pp. 638–643, 1987.
- Raffel, C., Shazeer, N., Roberts, A., Lee, K., Narang, S., Matena, M., Zhou, Y., Li, W., and Liu, P. J. Exploring the limits of transfer learning with a unified text-to-text transformer. *Journal of machine learning research*, 21 (140):1–67, 2020.
- Rumelhart, D. E., Hinton, G. E., and Williams, R. J. Learning representations by back-propagating errors. *nature*, 323(6088):533–536, 1986.
- Saha, R., Srivastava, V., and Pilanci, M. Matrix compression via randomized low rank and low precision factorization. *Advances in Neural Information Processing Systems*, 36, 2023.
- Sakaguchi, K., Bras, R. L., Bhagavatula, C., and Choi, Y. Winogrande: An adversarial winograd schema challenge at scale. *Communications of the ACM*, 64(9):99–106, 2021.
- Santos, C. F. G. D. and Papa, J. P. Avoiding overfitting: A survey on regularization methods for convolutional neural networks. *ACM Computing Surveys (CSUR)*, 54 (10s):1–25, 2022.
- Shridhar, K., Stolfo, A., and Sachan, M. Distilling reasoning capabilities into smaller language models. *arXiv preprint arXiv:2212.00193*, 2022.
- Song, J., Oh, K., Kim, T., Kim, H., Kim, Y., and Kim, J.-J. Sleb: Streamlining llms through redundancy verification and elimination of transformer blocks. *arXiv preprint arXiv:2402.09025*, 2024.
- Sun, M., Liu, Z., Bair, A., and Kolter, J. Z. A simple and effective pruning approach for large language models. *arXiv preprint arXiv:2306.11695*, 2023.
- Tao, C., Hou, L., Bai, H., Wei, J., Jiang, X., Liu, Q., Luo, P., and Wong, N. Structured pruning for efficient generative pre-trained language models. In *Findings of the Association for Computational Linguistics: ACL 2023*, pp. 10880–10895, 2023.
- Taori, R., Gulrajani, I., Zhang, T., Dubois, Y., Li, X., Guestrin, C., Liang, P., and Hashimoto, T. B. Stanford alpaca: An instruction-following llama model. https://github.com/tatsu-lab/stanford_alpaca, 2023.
- Tibshirani, R. Regression shrinkage and selection via the lasso. *Journal of the Royal Statistical Society Series B: Statistical Methodology*, 58(1):267–288, 1996.
- Touvron, H., Lavril, T., Izacard, G., Martinet, X., Lachaux, M.-A., Lacroix, T., Rozière, B., Goyal, N., Hambro, E., Azhar, F., et al. Llama: Open and efficient foundation language models. *arXiv preprint arXiv:2302.13971*, 2023.
- van der Ouderaa, T. F., Nagel, M., Van Baalen, M., Asano, Y. M., and Blankevoort, T. The llm surgeon. *arXiv preprint arXiv:2312.17244*, 2023.
- Vaswani, A. Attention is all you need. *Advances in Neural Information Processing Systems*, 2017.
- Wang, Z. Sparsert: Accelerating unstructured sparsity on gpus for deep learning inference. In *Proceedings of the ACM international conference on parallel architectures and compilation techniques*, pp. 31–42, 2020.
- Wen, W., Wu, C., Wang, Y., Chen, Y., and Li, H. Learning structured sparsity in deep neural networks. *Advances in neural information processing systems*, 29, 2016.

- Wolf, T. Huggingface’s transformers: State-of-the-art natural language processing. *arXiv preprint arXiv:1910.03771*, 2019.
- Wu, J., Feng, M., Zhang, S., Che, F., Wen, Z., and Tao, J. Beyond examples: High-level automated reasoning paradigm in in-context learning via mcts, 2024. URL <https://arxiv.org/abs/2411.18478>.
- Xia, H., Zheng, Z., Li, Y., Zhuang, D., Zhou, Z., Qiu, X., Li, Y., Lin, W., and Song, S. L. Flash-llm: Enabling cost-effective and highly-efficient large generative model inference with unstructured sparsity. *arXiv preprint arXiv:2309.10285*, 2023a.
- Xia, M., Gao, T., Zeng, Z., and Chen, D. Sheared llama: Accelerating language model pre-training via structured pruning. *arXiv preprint arXiv:2310.06694*, 2023b.
- Xiao, G., Lin, J., Seznec, M., Wu, H., Demouth, J., and Han, S. Smoothquant: Accurate and efficient post-training quantization for large language models. In *International Conference on Machine Learning*, pp. 38087–38099. PMLR, 2023.
- Xu, P., Shao, W., Chen, M., Tang, S., Zhang, K., Gao, P., An, F., Qiao, Y., and Luo, P. Besa: Pruning large language models with blockwise parameter-efficient sparsity allocation. *arXiv preprint arXiv:2402.16880*, 2024.
- Yang, Y., Cao, Z., and Zhao, H. Laco: Large language model pruning via layer collapse. *arXiv preprint arXiv:2402.11187*, 2024.
- Yao, Z., Yazdani Aminabadi, R., Zhang, M., Wu, X., Li, C., and He, Y. Zeroquant: Efficient and affordable post-training quantization for large-scale transformers. *Advances in Neural Information Processing Systems*, 35: 27168–27183, 2022.
- Yin, L., Wu, Y., Zhang, Z., Hsieh, C.-Y., Wang, Y., Jia, Y., Li, G., Jaiswal, A., Pechenizkiy, M., Liang, Y., et al. Outlier weighed layerwise sparsity (owl): A missing secret sauce for pruning llms to high sparsity. *arXiv preprint arXiv:2310.05175*, 2023.
- Zellers, R., Holtzman, A., Bisk, Y., Farhadi, A., and Choi, Y. Hellaswag: Can a machine really finish your sentence? *arXiv preprint arXiv:1905.07830*, 2019.
- Zhang, S., Roller, S., Goyal, N., Artetxe, M., Chen, M., Chen, S., Dewan, C., Diab, M., Li, X., Lin, X. V., et al. Opt: Open pre-trained transformer language models. *arXiv preprint arXiv:2205.01068*, 2022.
- Zhang, Y., Bai, H., Lin, H., Zhao, J., Hou, L., and Canistraci, C. V. Plug-and-play: An efficient post-training pruning method for large language models. In *The Twelfth International Conference on Learning Representations*, 2024.
- Zhou, A., Ma, Y., Zhu, J., Liu, J., Zhang, Z., Yuan, K., Sun, W., and Li, H. Learning n: m fine-grained structured sparse neural networks from scratch. *arXiv preprint arXiv:2102.04010*, 2021.
- Zhu, X., Li, J., Liu, Y., Ma, C., and Wang, W. A survey on model compression for large language models. *Transactions of the Association for Computational Linguistics*, 12:1556–1577, 2024.

A. Proofs of the Propositions

A.1. Proof of Proposition 3.1

Let us first assume that $A \in \mathbb{R}^{m \times n}$ and $B \in \mathbb{R}^{n \times k}$. We can express A as $[\mathbf{a}_1 \ \mathbf{a}_2 \ \dots \ \mathbf{a}_n]$, where $\mathbf{a}_i \in \mathbb{R}^{m \times 1}$, and B

as $\begin{bmatrix} \mathbf{b}_1^T \\ \mathbf{b}_2^T \\ \vdots \\ \mathbf{b}_n^T \end{bmatrix}$, where $\mathbf{b}_i \in \mathbb{R}^{k \times 1}$. Then, we obtain $C \in \mathbb{R}^{m \times k}$ as shown in Equation 11. It is important to note that the final summation in Equation 11 refers to the summation of n rank-1 matrices, not a scalar summation.

$$C = AB = [\mathbf{a}_1 \ \mathbf{a}_2 \ \dots \ \mathbf{a}_n] \times \begin{bmatrix} \mathbf{b}_1^T \\ \mathbf{b}_2^T \\ \vdots \\ \mathbf{b}_n^T \end{bmatrix} = \sum_{i=1}^n \mathbf{a}_i \mathbf{b}_i^T \quad (11)$$

According to Equation 11, when some columns of A are zero, the rows of B that correspond to the outer product with the zero columns of A can take any values, as the product of zero and any value is zero. These rows can therefore be set to zero.

Applying the above conclusion to the parameters of a transformer layer, if certain columns of W_{down}^{i-1} in the FFN layer of the $(i-1)$ th transformer layer are pruned, then, since W_Q^i , W_K^i , and W_V^i in the i th transformer layer are immediately multiplied by the result of W_{down}^{i-1} , the corresponding rows in W_Q^i , W_K^i , and W_V^i can be set to zero. Additionally, if certain columns of W_o^i in the i th transformer layer are pruned, the W_{up}^i in the FFN block will immediately multiply with it, so the corresponding rows in W_{up}^i should also be pruned. Thus, we have completed the proof of Proposition 3.1.

A.2. Proof of Proposition 3.2

Step 1: Expressing ℓ_1 -norm Using Elements.

The objective function in the unconstrained problem is the ℓ_1 -norm of the vector x , which is defined as:

$$\|x\|_1 = \sum_{i=1}^n |x_i| \quad (12)$$

This function aims to minimize the sum of the absolute values of the components of x .

Step 2: Reformulating the Constrained Problem

The constrained optimization problem introduces an auxiliary variable y , where for each element i :

$$x_i \geq -y_i \quad \text{and} \quad x_i \leq y_i \quad (13)$$

This implies that $y_i \geq |x_i|$, meaning each element of y serves as an upper bound for the absolute value of the corresponding element in x . Consequently, minimizing $\|x\|_1$ is equivalent to minimizing the sum of the elements in y . Thus, the objective function is defined as:

$$\mathbf{1}^T y \quad (14)$$

Thus, minimizing $\mathbf{1}^T y$ is equivalent to minimizing the sum of the absolute values of x , which is the ℓ_1 -norm of x .

This transformation allows the optimization problem to be solved without directly involving the absolute value function, resulting in an equivalent constrained optimization problem that can be addressed via backpropagation. Thus, the proof of the Proposition 3.2 is complete.

B. Detailed Implementation

In this part, we first introduce several hyperparameter settings, with the detailed results shown in Table 7. In our experiments, we employ FP16 precision for all evaluated models, including Phi-2, OPT-2.7B, OPT-6.7B, OPT-13B, LLaMA2-7B, and LLaMA2-13B. For all RFT configurations, we set the LoRA rank r to 32, the scaling factor α to 10, and the sequence length to 2048. All other hyperparameters follow the default settings provided in the Hugging Face PEFT package (Mangrulkar et al., 2022). Due to limited computational resources, we set the batch size to 64. In future work, we will further explore the impact of a broader range of batch sizes on the performance of the pruning method. These choices ensure a balance between model adaptability and computational efficiency, leveraging parameter-efficient fine-tuning while maintaining stable optimization dynamics.

Table 7. Implementation Details

Precision	LoRA Rank	Scaling Factor	Max Sequence Length	Batch Size	Learning Rate	Early Stop Threshold	Min Delta
FP16	32	10	2048	64	2e-5	5	1e-4

To ensure a fair comparison between DReSS and other methods, we maintain consistency in the data used across all approaches. Specifically, the data used by DReSS for regularization, by LLM Surgeon for periodic updates of model weights and structures, by SliceGPT for selecting channel importance, and by SLEB for identifying crucial transformer layers are identical. Furthermore, we ensure that the data employed during the RFT process is consistent across all methods, thereby enabling a controlled and equitable evaluation framework. Following previous works (Ashkboos et al., 2024; Song et al., 2024), for the comparison unstructured pruning methods like Mangniude, Wanda, and SparseGPT, we ensure that the data used to compute the importance of individual weights is the same as the data used by DReSS for regularization.

C. Results of Comparison with Unstructured Pruning Methods

We compare DReSS at a 25% pruning ratio with unstructured pruning methods employing 2:4 sparsity (where two out of every four consecutive parameters are set to zero) and present the experimental results in Table 8. For unstructured pruning methods, only calibration data is required. To ensure consistency, all methods utilize a total of 1,000 samples, randomly selected from WikiText-2. The models used in these experiments consists of the OPT and LLaMA model families.

Compare to structured pruning methods, the primary advantage of unstructured pruning lies in its flexibility, enabling the removal of specific weights while preserving critical information in the remaining parameters of LLMs. Based on the results in Table 8, it can be seen that DReSS with a pruning ratio of 25% significantly outperforms existing unstructured pruning methods with a sparsity of 2:4 on generative and zero-shot tasks, demonstrating the powerful performance of DReSS. The reason DReSS outperforms unstructured pruning in comparisons lies in the regularization process before pruning. This process transfers important information hidden in the parameter space to the remaining parts of the model, preventing irreversible performance degradation caused by direct pruning and the resulting loss of information.

Table 8. Performance comparison with unstructured pruning methods. ‘PPL’ refers to the perplexity on WikiText-2. The accuracy is reported on five zero-shot tasks: PIQA, WinoGrande, HellaSwag, ARC-e, and ARC-c, as well as the average accuracy. The best result is highlighted in **bold**, and the second-best in underlined. DReSS- ℓ_2 denotes the use of the ℓ_2 -norm, while DReSS- ℓ_1 denotes the use of the ℓ_1 -norm.

Model	Method	Pruning Ratio	PPL (\downarrow)	PIQA	WinoGrande	HellaSwag	ARC-e	ARC-c	Avg_Acc
OPT-2.7B	Dense	0%	12.46	74.81	61.01	60.58	54.42	31.14	56.39
	Magnitude	2:4	265	57.46	42.19	35.62	32.58	16.42	36.85
	Wanda	2:4	16.54	64.32	57.84	41.63	43.47	23.44	46.14
	SparseGPT	2:4	13.48	68.58	56.72	45.36	46.89	25.92	48.69
	DReSS- ℓ_2	25%	12.52	69.12	58.98	49.10	50.62	28.15	51.20
	DReSS- ℓ_1	25%	12.48	<u>68.89</u>	<u>58.33</u>	<u>48.62</u>	51.67	<u>27.55</u>	<u>51.01</u>
OPT-6.7B	Dense	0%	10.85	76.39	65.19	67.16	60.14	34.64	60.70
	Magnitude	2:4	969	62.16	48.74	43.48	41.57	20.63	43.32
	Wanda	2:4	13.29	71.76	60.22	54.20	51.18	28.33	53.14
	SparseGPT	2:4	11.55	74.21	60.77	57.25	53.03	29.44	54.94
	DReSS- ℓ_2	25%	11.06	74.26	<u>63.12</u>	61.26	56.64	<u>31.77</u>	57.41
	DReSS- ℓ_1	25%	11.74	73.86	64.28	<u>60.45</u>	<u>56.36</u>	32.07	<u>57.40</u>
OPT-13B	Dense	0%	10.12	76.82	64.80	69.81	61.87	35.67	61.79
	Magnitude	2:4	1.2e4	64.38	52.19	49.46	44.58	21.25	46.37
	Wanda	2:4	13.49	72.25	61.72	57.97	53.96	29.69	55.12
	SparseGPT	2:4	11.17	74.16	62.43	59.18	56.27	31.74	56.76
	DReSS- ℓ_2	25%	10.38	74.06	64.57	66.82	61.56	35.33	60.47
	DReSS- ℓ_1	25%	<u>10.56</u>	73.65	<u>64.38</u>	<u>66.46</u>	<u>61.15</u>	<u>34.74</u>	<u>60.07</u>
LLaMA2-7B	Dense	0%	5.47	79.11	69.06	75.99	74.58	46.25	69.00
	Magnitude	2:4	54.59	64.42	60.93	56.72	59.18	27.31	53.71
	Wanda	2:4	11.35	70.84	62.27	55.33	57.58	31.91	55.59
	SparseGPT	2:4	8.67	72.14	64.96	58.93	60.90	34.22	58.23
	DReSS- ℓ_2	25%	<u>5.86</u>	<u>73.18</u>	66.49	<u>61.73</u>	65.42	40.86	61.54
	DReSS- ℓ_1	25%	5.81	73.42	<u>65.73</u>	61.92	<u>65.26</u>	<u>39.68</u>	<u>61.20</u>
LLaMA2-13B	Dense	0%	4.88	80.47	72.22	79.39	77.48	49.23	71.76
	Magnitude	2:4	8.33	70.47	62.04	50.65	62.46	31.74	55.47
	Wanda	2:4	8.32	73.94	67.01	63.09	64.31	37.80	61.23
	SparseGPT	2:4	7.07	75.46	68.51	65.52	66.04	39.76	63.06
	DReSS- ℓ_2	25%	5.12	76.14	71.22	<u>76.51</u>	<u>73.45</u>	46.87	68.84
	DReSS- ℓ_1	25%	<u>5.16</u>	77.24	<u>70.61</u>	76.75	73.84	<u>45.46</u>	<u>68.78</u>

D. Changes in the Parts Without Regularization

As illustrated in Figure 6, the magnitude of the unregularized parameters exhibits an increase after the application of regularization, suggesting a redistribution of model capacity. This phenomenon indicates that during regularization, critical information, initially encoded in the regularized portion of the model, is partially transferred to the unregularized portion. In contrast, Figure 3 shows a reduction in the magnitude of the regularized parameters after regularization, implying that the imposed constraints effectively suppress the corresponding parameter values, enforcing sparsity or compression in that region.

Collectively, these observations suggest that the regularization process facilitates an implicit redistribution of information across different parameter subsets. Specifically, the regularization term promotes a shift of important model characteristics from the constrained (regularized) portion to the unconstrained (unregularized) portion, thereby preserving essential model knowledge despite the imposed sparsity constraints. Based on this insight, we posit that pruning the regularized portion post-regularization could mitigate information loss, as the core knowledge has already been migrated to the unregularized segment. This pruning strategy effectively reduces parameter redundancy while retaining the model’s language modeling capacity, thereby achieving a more compact and efficient representation without compromising performance.

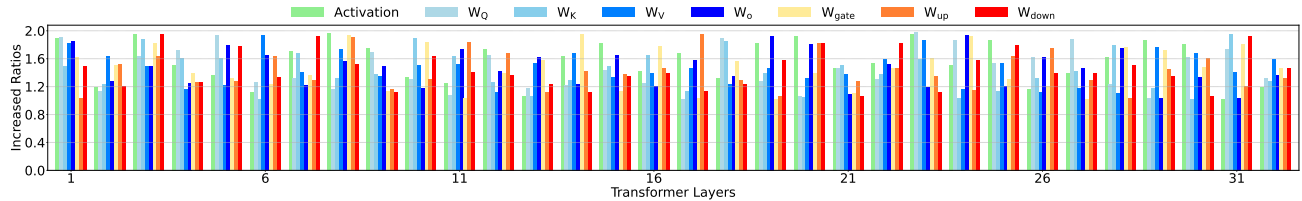


Figure 6. Ratio of the sum of absolute values of unregularized parameters after LLaMA2-7B regularization to the sum of absolute values of the corresponding parameters before regularization. For example, regularization is not applied to the first 75% of rows in W_Q , and the absolute sum of the rows after regularization is divided by the sum of the corresponding rows before regularization to obtain the Increased Ratios. This is applied similarly to other matrices such as W_K , W_V , W_O , W_{gate} , W_{up} , W_{down} , and for layer activations X , the sum of the unregularized columns is compared to the original sum.

E. Performance of DReSS under Different Pruning Ratios and Datasets

E.1. The Perplexity of DReSS under Different Pruning Ratios and Datasets

In Section 4.2, we utilize 1,000 samples randomly selected from the WikiText-2 dataset to guide the regularization process. Subsequently, we evaluate multiple large language models (LLMs) by measuring changes in perplexity across various generative task datasets, including WikiText-2, Alpaca, PTB, and C4, under pruning rates of 10%, 20%, 30%, 40%, 50%, and 60%. The detailed results, presented in Table 9, indicate that DReSS exhibits greater robustness as model scale increases, suggesting that the proposed method effectively mitigates performance degradation in larger architectures. This highlights the scalability of DReSS and its potential to maintain model efficiency under varying levels of sparsity.

Table 9. Perplexity comparison of DReSS with different pruning ratios. We set the pruning ratios to 10%, 20%, 30%, 40%, 50%, and 60%, and test the perplexity of the OPT and LLaMA2 models on the generation task datasets Alpaca, WikiText-2, PTB, and C4. For DReSS, we use the ℓ_2 -norm.

Model	Pruning Ratio	WikiText-2	Alpaca	PTB	C4
OPT-2.7B	Dense	12.46	11.64	17.97	14.32
	10%	12.48	11.71	18.16	14.71
	20%	12.51	11.93	19.45	15.42
	30%	14.49	12.88	23.58	18.93
	40%	18.92	15.46	31.30	24.33
	50%	24.57	21.37	45.32	32.15
	60%	33.83	31.22	58.73	45.56
OPT-6.7B	Dense	10.85	10.27	15.77	12.71
	10%	10.91	10.45	16.05	13.18
	20%	11.02	10.83	17.58	14.45
	30%	12.32	11.46	19.65	16.68
	40%	14.26	12.71	25.52	20.94
	50%	19.63	15.66	33.78	28.22
	60%	28.75	21.39	47.29	39.47
OPT-13B	Dense	10.12	9.46	14.52	12.06
	10%	10.26	9.65	14.88	12.37
	20%	10.47	9.97	15.64	13.15
	30%	10.99	10.56	18.81	15.63
	40%	11.62	11.25	23.07	19.55
	50%	16.15	14.68	29.26	26.21
	60%	27.63	20.12	38.59	35.58
LLaMA2-7B	Dense	5.47	5.25	7.92	7.26
	10%	5.54	5.29	8.06	7.34
	20%	5.63	5.37	8.29	7.79
	30%	7.39	7.32	9.13	8.46
	40%	9.62	8.62	12.37	10.56
	50%	13.77	12.59	18.85	15.18
	60%	24.38	20.25	29.34	27.37
LLaMA2-13B	Dense	4.88	4.63	7.16	6.73
	10%	4.94	4.69	7.23	6.96
	20%	5.08	4.83	7.61	7.53
	30%	5.61	5.42	8.33	8.14
	40%	6.25	6.14	9.27	9.05
	50%	7.59	7.28	11.58	10.88
	60%	12.77	11.78	15.16	13.62

E.2. The Accuracy of DReSS under Different Pruning Ratios on Zero-shot Tasks

To systematically evaluate the performance of DReSS on zero-shot tasks under varying pruning rates, we adopt the experimental setup outlined in Section 4.2, where 1,000 samples are randomly selected from the WikiText-2 dataset to guide the regularization process. We assess the accuracy of different model configurations at pruning rates of 10%, 20%, 30%, 40%, 50%, and 60% across a diverse set of benchmark datasets, including PIQA, WinoGrande, HellaSwag, ARC-e, and ARC-c. The results, summarized in Table 10, provide insights into the impact of sparsity on zero-shot generalization. Notably, the analysis reveals that DReSS maintains competitive performance even at higher pruning rates, demonstrating its effectiveness in preserving reasoning and commonsense understanding across different tasks.

Table 10. Accuracy comparison of DReSS with different pruning ratios. We set the pruning ratios to 10%, 20%, 30%, 40%, 50%, and 60%, and test the accuracy of the OPT and LLaMA2 models on the zero-shot task datasets PIQA, WinoGrande, HellaSwag, ARC-e and ARC-c. For DReSS, we use the ℓ_2 -norm. ‘Avg_Acc’ represents the average accuracy.

Model	Pruning Ratio	PIQA	WinoGrande	HellaSwag	ARC-e	ARC-c	Avg_Acc
OPT-2.7B	Dense	74.81	61.01	60.58	54.42	31.14	56.39
	10%	70.38	60.12	51.79	52.46	29.78	52.91
	20%	69.96	59.47	50.45	51.87	28.62	52.07
	30%	64.52	58.76	49.25	50.23	27.52	50.06
	40%	61.32	56.27	47.39	48.26	25.57	47.76
	50%	59.38	53.46	44.63	46.19	21.66	45.06
	60%	52.99	48.74	40.03	43.35	16.25	40.27
OPT-6.7B	Dense	76.39	65.19	67.16	60.14	34.64	60.70
	10%	75.89	64.61	64.69	58.53	33.47	59.44
	20%	75.12	64.23	62.56	57.34	32.95	58.44
	30%	72.52	62.63	58.27	54.48	29.99	55.58
	40%	67.37	58.59	52.12	49.38	26.87	50.87
	50%	61.48	55.62	46.46	47.68	22.97	46.84
	60%	55.73	51.52	43.38	45.85	18.62	43.02
OPT-13B	Dense	76.82	64.80	69.81	61.87	35.67	61.79
	10%	75.46	64.69	68.56	61.79	35.58	61.22
	20%	74.78	64.61	67.25	61.66	35.43	60.75
	30%	72.62	63.26	65.69	59.64	32.57	58.76
	40%	68.67	61.49	62.74	55.98	29.26	55.63
	50%	62.19	56.46	58.55	52.15	24.53	50.78
	60%	57.43	52.72	51.23	47.62	21.05	46.01
LLaMA2-7B	Dense	79.11	69.06	75.99	74.58	46.25	69.00
	10%	77.38	68.16	71.28	69.26	43.73	65.96
	20%	76.42	67.35	68.26	66.73	41.68	64.09
	30%	72.29	64.87	58.53	63.48	39.27	59.69
	40%	68.66	61.49	55.42	58.61	36.52	56.14
	50%	61.32	55.68	51.79	52.35	31.55	50.54
	60%	56.45	51.79	48.96	48.98	27.26	46.69
LLaMA2-13B	Dense	80.47	72.22	79.39	77.48	49.23	71.76
	10%	79.35	72.15	76.42	76.92	48.57	70.68
	20%	78.27	71.98	73.20	75.43	47.62	69.30
	30%	75.49	69.73	71.54	72.87	45.41	67.00
	40%	73.56	64.46	67.75	68.45	41.28	63.10
	50%	68.73	59.82	62.48	60.12	36.14	57.46
	60%	62.25	56.27	59.93	53.37	29.77	52.32

F. More Details of the Dependency on Calibration Dataset

When using Alpaca, WikiText-2, C4, and PTB as calibration and RFT data, the perplexity of various methods on Alpaca, C4, and PTB is shown as follows:

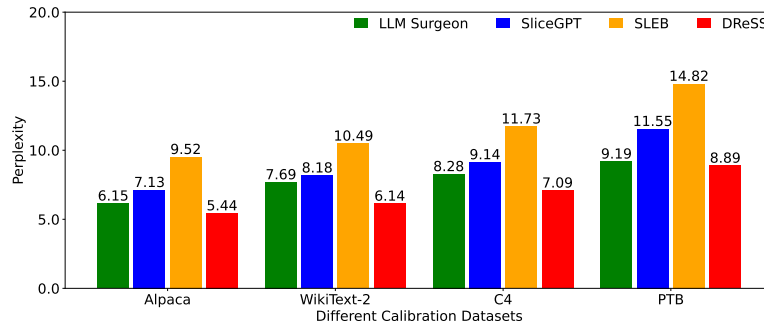


Figure 7. Comparison of perplexity on Alpaca using different calibration datasets at a pruning ratio of 25% on LLaMA2-7B.

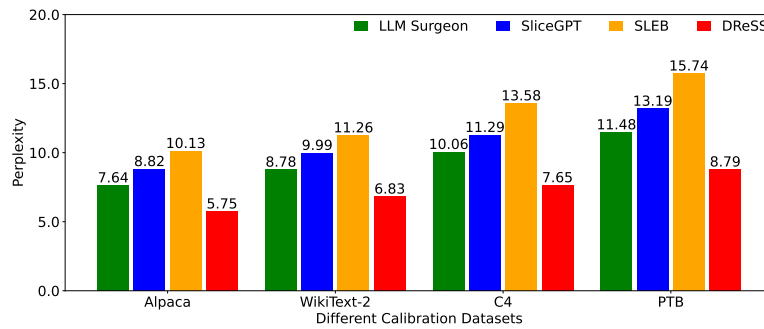


Figure 8. Comparison of perplexity on C4 using different calibration datasets at a pruning ratio of 25% on LLaMA2-7B.

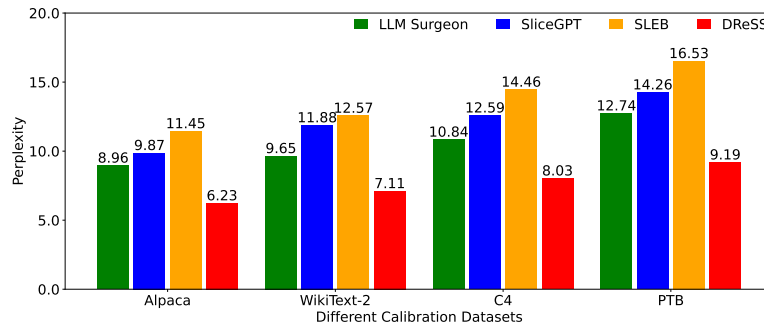


Figure 9. Comparison of perplexity on PTB using different calibration datasets at a pruning ratio of 25% on LLaMA2-7B.